

LPT-Orsay 03-99

IPPP/03/76

DCPT/03/152

Isolated photon + jet photoproduction as a tool to constrain the gluon distribution in the proton and the photon

M. Fontannaz^(a), G. Heinrich^{(b),1}

^(a) *Laboratoire de Physique Théorique, UMR 8627 CNRS, Université Paris XI, Bâtiment 210, 91405 Orsay Cedex, France*

^(b) *IPPP, Department of Physics, University of Durham, Durham DH1 3LE, England*

Abstract

We analyse how the reaction $\gamma p \rightarrow \gamma + \text{jet} + X$ can serve to constrain the gluon distributions. Our results are based on a code of partonic event generator type which includes full NLO corrections. We conclude that there are phase space domains in which either the gluon in the photon or the gluon in the proton give important contributions to the cross section, which should be observable in HERA experiments.

¹Address after December 1, 2003: II. Institut für Theoretische Physik, Universität Hamburg, Luruper Chaussee 149, 22761 Hamburg, Germany.

1 Introduction

Over the past years, the ZEUS [1, 2] and H1 [3] collaborations at HERA have been able to observe the photoproduction of large- p_T photons, and the comparisons of data with existing NLO QCD predictions [4, 5, 6, 7, 8] appear successful. In photoproduction reactions, a quasi-real photon, emitted at small angle from the electron, interacts with a parton from the proton. The photon can either participate directly in the hard scattering or be resolved into a partonic system, in which case the parton stemming from the photon takes part in the hard interaction. Therefore photoproduction is a privileged reaction to measure or constrain the parton distributions in the photon and in the proton. In this paper we shall investigate the possibility to constrain both the gluon in the photon and the gluon in the proton by looking at the production of a large- p_T photon and a jet. With the aim of enhancing the contribution of processes involving initial gluons, we will explore various kinematical domains in detail. We shall show that there are kinematical configurations which are dominated either by the gluon in the photon, or by the gluon in the proton, and which should be accessible to experiment.

The photoproduction of large- p_T particles and jets has a long story; it offers interesting tests of QCD and gives access to the measurement of the initial state parton distributions and the final state fragmentation functions (for a review, see e.g. [9]). Reactions involving large- p_T jets and/or hadrons have been copiously observed because of their large cross sections, whereas the production of prompt photons has been measured only more recently and the statistical errors are still rather large. However, this latter reaction has advantages with respect to jet or hadron production. Indeed a large transverse momentum is necessary to unambiguously define a jet and to avoid too large hadronisation and underlying events corrections. The theoretical predictions also are subject to uncertainties due to scale variations. All these effects are quite sizeable, even for $E_T^{\text{jet}} > 21$ GeV [10]. The photoproduction of large- p_T hadrons also suffers from sizeable theoretical uncertainties coming from a large sensitivity to scale variations and from the fragmentation functions which are not very accurately measured [11, 12]. In the case of a large- p_T photon, there is of course no problem due to jet definition, hadronisation or inaccurate fragmentation functions (only isolated photons are observed). Even more importantly, the theoretical predictions are reasonably stable under scale variations. Therefore the photoproduction of prompt photons appears as an ideal reaction to test QCD and measure the non-perturbative inputs.

However one must keep in mind two reserves, one of experimental and another one of theoretical nature. First, the measured cross sections are small and become rapidly very low at peripheral regions of the phase space which might be physically interesting. Moreover, the detection of a photon among the huge amount of large- p_T π^0 's is not an easy task. Second, only isolated photons are observed, the isolation criterion being that very little hadronic energy is contained in a cone surrounding

the photon. This has the advantage of reducing the fragmentation component of the cross section, but at the same time this isolation can eliminate events containing too much hadronic energy coming from the underlying event in the cone, an effect which cannot be taken into account in the NLO calculations. This point has been discussed in [6] and studied by the H1 collaboration [3, 13].

In order to constrain the kinematics of the different subprocesses, it is important to observe a large- p_T jet in association with the photon, which introduces uncertainties in the comparison between data and theory due to hadronisation and underlying event phenomena. However, the effect of these phenomena can be considerably reduced if the transverse momentum of the jet, which is not well measured, is not used to constrain the kinematics, but only its rapidity. This is done by using the variables x_{LL} [14, 6] instead of the commonly used x_{obs} . We will make an extensive use of the variables x_{LL} for the proton and the photon in order to constrain the kinematical region relevant for the observation of the gluon distributions.

Our paper is organised in the following way. In Section 2, we discuss theoretical issues related to the subsequent numerical studies, such as photon isolation, suitable observables to study the parton distributions and the importance of asymmetric cuts on the minimum transverse energies. Section 3 contains the numerical results, where first the sensitivity to the gluon content of the proton is studied. Then we turn to the gluon distribution in the real photon before we conclude in Section 4.

2 Theoretical framework

As the general framework of the calculation already has been described in detail in [5, 6], we will sketch the method only briefly here and focus instead on issues related to the gluon distributions.

In photoproduction, the electron acts like a source of quasi-real photons whose spectrum can be described by the Weizsäcker-Williams approximation, which we use in the following form

$$f_\gamma^e(y) = \frac{\alpha_{em}}{2\pi} \left\{ \frac{1 + (1-y)^2}{y} \ln \frac{Q_{\max}^2(1-y)}{m_e^2 y^2} - \frac{2(1-y)}{y} \right\}. \quad (1)$$

As already mentioned, the quasi-real photon then either takes part *directly* in the hard scattering process, or it acts as a composite object, being a source of partons which take part in the hard subprocess. The latter mechanism is referred to as *resolved* process and is parametrised by the parton distributions in the photon $F_{a/\gamma}(x^\gamma, Q^2)$. Thus the distribution of partons of type "a" in the electron is a convolution

$$F_{a/e}(x_e, M) = \int_0^1 dy dx^\gamma f_\gamma^e(y) F_{a/\gamma}(x^\gamma, M) \delta(x^\gamma y - x_e) \quad (2)$$

where in the "direct" case the parton a is the photon itself, i.e. $F_{a/\gamma}(x^\gamma, M) = \delta_{a\gamma} \delta(1-x^\gamma)$. The parton distributions in the photon $F_{a/\gamma}(x, Q^2)$ behave like $\alpha/\alpha_s(Q^2)$ for large

Q^2 . Therefore the additional power of α_s contained in the "resolved" component as compared to the "direct" one is compensated. This means that the NLO corrections to the resolved component can be numerically sizeable and have to be taken into account.

The cross section can symbolically be written as

$$\begin{aligned}
d\sigma^{ep\rightarrow\gamma j}(P_e, P_p, P_\gamma, P_j) &= \\
\sum_{a,b} \int dx_e \int dx_p F_{a/e}(x_e, M) F_{b/p}(x_p, M) \{d\hat{\sigma}^{\text{dir}} + d\hat{\sigma}^{\text{frag}}\} & \quad (3) \\
d\hat{\sigma}^{\text{dir}} &= d\hat{\sigma}^{ab\rightarrow\gamma j}(x_a, x_b, P_\gamma, P_j, \mu, M, M_F) \\
d\hat{\sigma}^{\text{frag}} &= \sum_c \int dz D_{\gamma/c}(z, M_F) d\hat{\sigma}^{ab\rightarrow cj}(x_a, x_b, P_\gamma/z, P_j, \mu, M, M_F)
\end{aligned}$$

where we have split the hard scattering cross sections $\hat{\sigma}$ explicitly into a "direct" and a "fragmentation" part in order to point out that there are two contributions to the "prompt photon" in the final state: The "direct" one, where the final state photon is produced directly in the hard interaction, and the one where the photon stems from the fragmentation of a large- p_T quark or gluon in the final state. This fragmentation process is described by the fragmentation functions $D_{\gamma/c}(z, M_F)$. At next-to-leading order, the distinction between "direct" and "fragmentation" becomes scheme dependent because the final state collinear singularity appearing in a "direct" process like $\gamma g \rightarrow \gamma q\bar{q}$ when a quark becomes collinear to the photon is absorbed at the fragmentation scale M_F into the "bare" fragmentation functions, and where to attribute the finite parts is a matter of choice of the factorisation scheme. In our calculation we use the $\overline{\text{MS}}$ scheme.

Note that the cross section (3) depends on three scales, the renormalisation scale μ , the initial state factorisation scale M , and the fragmentation scale M_F , and that it can be considered as consisting of 4 categories of subprocesses, depending on whether there is a "direct" photon in the initial and/or final state: 1. direct direct, 2. resolved direct, 3. direct fragmentation, 4. resolved fragmentation. Each of these contributions consists of several partonic subprocesses at NLO and is strongly scale dependent. Only in the sum this scale dependence cancels to a large extent, and only the sum can be considered as a physical quantity. This has to be kept in mind when the contributions of certain subprocesses only will be considered below, in order to estimate the contribution of gluon initiated processes. The study of particular subprocesses can be very useful to get an idea of the underlying parton dynamics, but cannot be considered as precise quantitative statements because of the scale and scheme dependence outlined above.

We would like to emphasize that we calculated the full NLO corrections to all four categories of subprocesses. We also included the quark loop box contribution $\gamma g \rightarrow \gamma g$ which is NNLO from a naive α_s power counting point of view, but as the process $\gamma g \rightarrow \gamma g$ does not exist at tree level, the box is the "leading order"

diagram for this process, and its numerical contribution is quite sizeable [5]. The calculation presented in [7, 8] has no higher order corrections to the resolved-direct, direct-fragmentation and resolved-fragmentation contributions. It only contains the higher order corrections to the direct-direct part, and the box contribution is also included.

Photon Isolation

In prompt photon measurements, the experimental challenge consists in the separation of prompt photon events from the large background of secondary photons produced by the decay of light mesons, predominantly π^0 mesons. The latter, when produced at high energy, decay into two almost collinear photons which cannot be resolved in the calorimeter. However, they are in general accompanied by hadronic energy and thus this background can be suppressed by isolation cuts.

Commonly a cone isolation criterion is used, defined in the following way²: A photon is isolated if, inside a cone centered around the photon direction in the rapidity and azimuthal angle plane, the amount of hadronic transverse energy E_T^{had} deposited is smaller than some value $E_{T,max}$ fixed by the experiment:

$$\begin{aligned} (\eta - \eta^\gamma)^2 + (\phi - \phi^\gamma)^2 &\leq R_{exp}^2 \\ E_T^{had} &\leq E_{T,max} . \end{aligned} \tag{4}$$

Following the HERA conventions, we used $E_{T,max} = \epsilon p_T^\gamma$ with $\epsilon = 0.1$ and $R_{exp} = 1$. Of course isolation not only reduces the background from secondary photons, but also substantially reduces the fragmentation components, such that the total cross section depends very little on the fragmentation functions.

But another, undesired, effect of isolation is a partial suppression of the direct contribution. Indeed, the hadronic transverse energy E_T^{had} deposited in the cone may stem from the soft underlying event due to the spectator-spectator collisions. This renders the effective isolation cut more stringent and leads to a decrease of the cross section, included the direct contributions. The simulation of this effect, discussed in [5], requires a good knowledge of the hadron distributions in the underlying event, which is asymmetric in γp collisions; it has been studied in recent H1 publications [3, 13].

²A more sophisticated criterion has been proposed in [15], in which the veto on accompanying hadronic transverse energy is the more severe, the closer the corresponding hadron is to the photon direction. It has been designed to make the fragmentation contribution vanish completely, in an infrared safe way, but is less straightforward to implement experimentally.

2.1 Suitable observables to study the parton distributions

As observables which serve to reconstruct the longitudinal momentum fraction of the parton stemming from the proton respectively photon, it is common to use

$$x_{obs}^p = \frac{p_T^\gamma e^{\eta^\gamma} + E_T^{\text{jet}} e^{\eta^{\text{jet}}}}{2E^p}, \quad x_{obs}^\gamma = \frac{p_T^\gamma e^{-\eta^\gamma} + E_T^{\text{jet}} e^{-\eta^{\text{jet}}}}{2E^\gamma}. \quad (5)$$

However, as the measurement of E_T^{jet} can be a substantial source of systematic errors at low E_T values, we propose a slightly different variable which does not depend on E_T^{jet} ,

$$x_{LL}^{p,\gamma} = \frac{p_T^\gamma (e^{\pm\eta^\gamma} + e^{\pm\eta^{\text{jet}}})}{2E^{p,\gamma}}. \quad (6)$$

At leading order, for the non-fragmentation contribution, the variables x_{obs} and x_{LL} coincide, and they are also equal to the "true" partonic longitudinal momentum fraction, i.e. the argument of the parton distribution function. At NLO, the real corrections involve 3 partons in the final state (with transverse momenta p_{T3}, p_{T4}, p_{T5}), one of which – say parton 5 – is unobserved. Therefore, x_{obs} and x_{LL} will be different at NLO.

The difference between x_{LL} and x_{obs} is rather small in the proton case, as shown in Fig. 1 a). In the photon case, x_{LL}^γ and x_{obs}^γ are very similar in the region $0 \lesssim x^\gamma \lesssim 0.85$. However, for x^γ close to one, there are important differences between x_{LL}^γ and x_{obs}^γ , the former leading to a smoother distribution $d\sigma/dx^\gamma$ if the size of the bins around $x^\gamma = 1$ is not chosen too small (see Fig. 1 b).

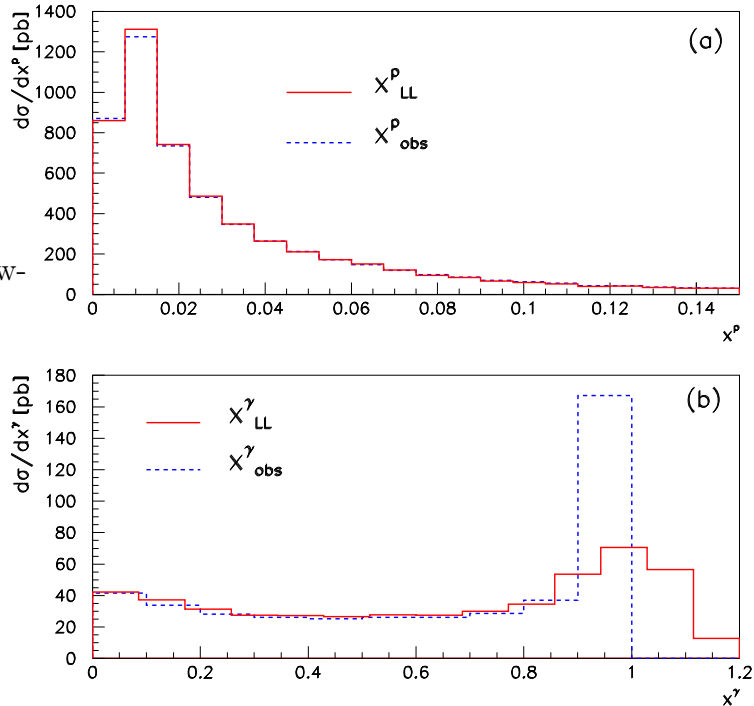


Figure 1: Comparison of x_{LL} and x_{obs} for the proton and the photon. The photon and jet rapidities and transverse energies have been integrated in the range $-2 \leq \eta^{\gamma,\text{jet}} \leq 4$, $p_T^\gamma \geq 6$ GeV, $E_T^{\text{jet}} \geq 5$ GeV, $\sqrt{s} = 318$ GeV.

2.2 Asymmetric cuts

It is well known [16, 14, 6] that symmetric cuts on the minimum transverse energies of dijets or a photon plus a jet should be avoided as they amount to including a region where the fixed order perturbative calculation shows infrared sensitivity. As explained in detail in [6], the problem stems from terms $\sim \log^2(|1 - p_T^\gamma/E_{T,\min}^{\text{jet}}|)$ which become large as p_T^γ approaches $E_{T,\min}^{\text{jet}}$, the lower cut on the jet transverse energy. Therefore the partonic NLO cross section has a singular behaviour at $p_T^\gamma = E_{T,\min}^{\text{jet}}$, which is displayed in Fig. 2. Of course, analogously, there are $\log^2(|1 - E_T^{\text{jet}}/p_{T,\min}^\gamma|)$ terms which become large for $E_T^{\text{jet}} \rightarrow p_{T,\min}^\gamma$, see Fig. 3.

The comparison with data can be done in two ways. First, if one wants to display e.g. the differential cross section $d\sigma/dE_T^{\text{jet}}$ while $p_{T,\min}^\gamma$ lies within the considered E_T^{jet} range, the binning in E_T^{jet} must be chosen large enough to average over the logarithmic singularity which is integrable. For instance, the binning $E_T^{\text{jet}} - \Delta \leq p_{T,\min}^\gamma \leq E_T^{\text{jet}} + \Delta$ with $\Delta = 0.5 \text{ GeV}$ for the bin around $p_{T,\min}^\gamma = 7 \text{ GeV}$ in Fig. 3 should lead to a correct average of the theoretical singularity and allow for a comparison with data. Obviously, $d\sigma/dp_T^\gamma$ will not exhibit a problem as long as $E_{T,\min}^{\text{jet}} < p_{T,\min}^\gamma$ since the critical point $p_T^\gamma = E_{T,\min}^{\text{jet}}$ will not be reached in this case.

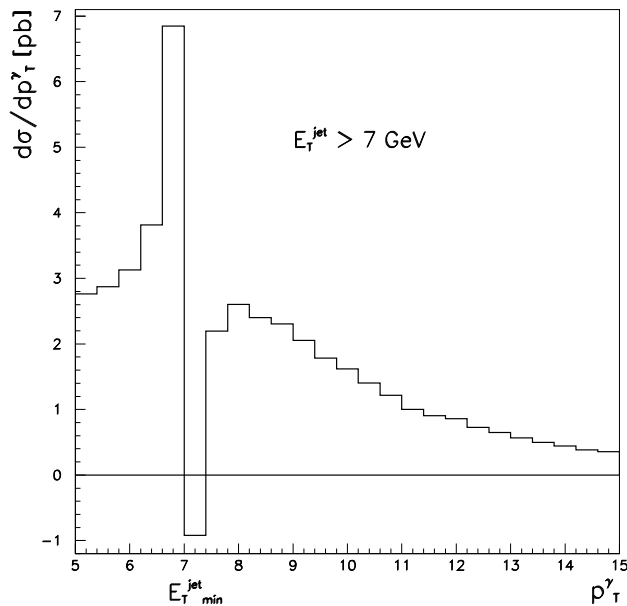


Figure 2: Logarithmic singularity in $d\sigma/dp_T^\gamma$ at $p_T^\gamma = E_{T,\min}^{\text{jet}}$.

Second, one often would like to have a more inclusive cross section such as $d\sigma/d\eta^\gamma$, obtained by integrating the differential cross section over p_T^γ and E_T^{jet} . In this case one should not choose $p_{T,\min}^\gamma = E_{T,\min}^{\text{jet}}$ as this amounts to integrating the spectrum of Fig. 3 to the right-hand side of $p_{T,\min}^\gamma$ only and thus to picking up only the singular negative contribution to the NLO cross section, without the compensation coming from the positive contribution to the left of $p_{T,\min}^\gamma$. As a result, the theoretical prediction, although being finite, is infrared sensitive as a consequence of choosing symmetric cuts. This point has been discussed in detail in ref. [6].

It is also illustrated in Fig. 4, where we consider the cross section $d\sigma/d\eta^{\text{jet}}$ in a kinematic range studied by H1. To exhibit the effect of different cuts on E_T^{jet} , we vary $E_{T,\text{min}}^{\text{jet}}$ to take the values 4, 4.5 or 5 GeV, while $p_{T,\text{min}}^{\gamma}$ has been fixed to 5 GeV, and display direct and resolved parts separately. Note that the leading order prediction is the same for all three values of $E_{T,\text{min}}^{\text{jet}}$ as E_T^{jet} cannot become smaller than $p_{T,\text{min}}^{\gamma}$ at leading order. One observes that in the direct part at small rapidities, the higher order corrections are large and negative. In the case of symmetric cuts, they are even negative in the resolved part at small rapidities, and the theoretical prediction depends strongly on the small change in $E_{T,\text{min}}^{\text{jet}}$ from 5 GeV to 4.5 GeV, whereas away from the symmetric cut region, the prediction is much more stable under small changes of $E_{T,\text{min}}^{\text{jet}}$.

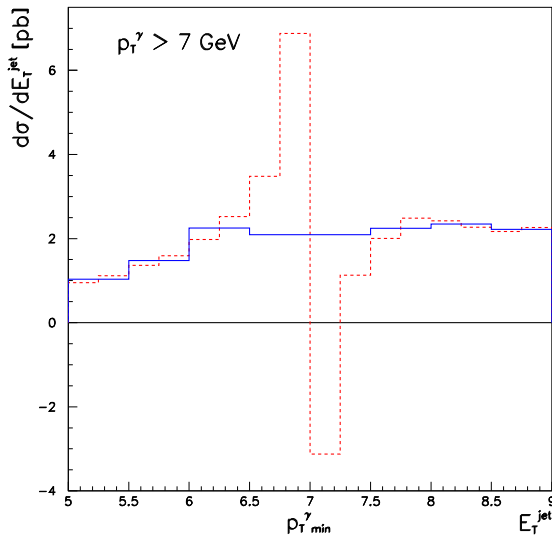


Figure 3: The logarithmic singularity in $d\sigma/dE_T^{\text{jet}}$ at $E_T^{\text{jet}} = p_{T,\text{min}}^{\gamma}$ is averaged over by choosing the binning large enough.

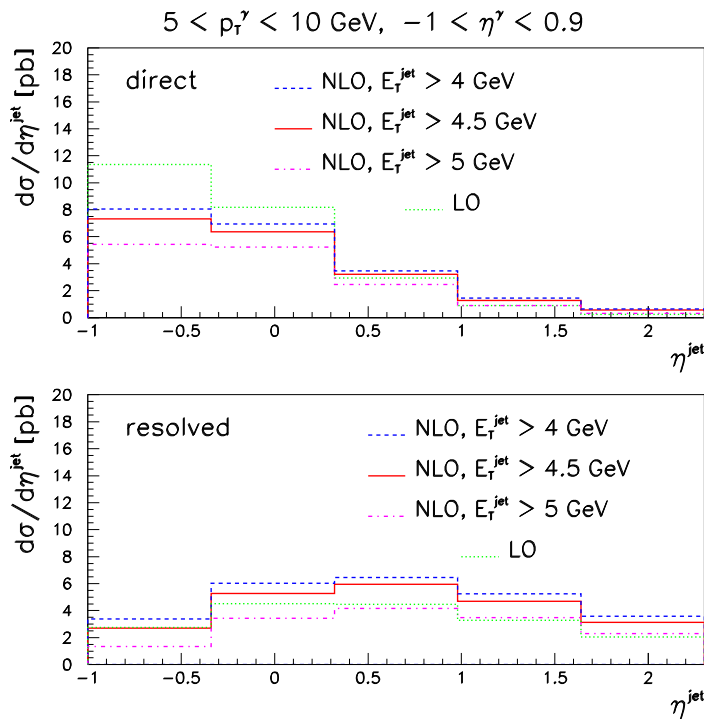


Figure 4: Magnitude of higher order corrections to direct/resolved parts separately

In summary, we repeat that for a successful comparison of data and NLO theory, one has to either ensure to stay away from IR singular domains or to consider suitably averaged observables. In what concerns the cuts on p_T^{γ} and E_T^{jet} , this amounts to choosing asymmetric cuts adapted to the observable. Therefore we disagree with the statement made in [17] that asymmetric cuts are not superior to symmetric ones.

3 Numerical results

Our studies are based on the program `EPHOX`³, which is a partonic Monte Carlo event generator. Unless stated otherwise, we use the following input for our numerical results: A center of mass energy $\sqrt{s} = 318 \text{ GeV}$ with $E_e = 27.5 \text{ GeV}$ and $E_p = 920 \text{ GeV}$ is used. The cuts on the minimum transverse energies of photon and jet are $E_T^{\text{jet}} > 5 \text{ GeV}$, $p_T^\gamma > 6 \text{ GeV}$. The rapidities have been integrated over in the domain $-2 \leq \eta^\gamma, \eta^{\text{jet}} \leq 4$ unless stated otherwise. For the parton distributions in the proton we take the MRST01 [18] parametrisation, for the photon we use AFG04⁴ [19] distribution functions and BFG [20] fragmentation functions. We take $n_f = 4$ flavours, and for $\alpha_s(\mu)$ we use an exact solution of the two-loop renormalisation group equation, and not an expansion in $\log(\mu/\Lambda)$. The default scale choice is $M = M_F = \mu = p_T^\gamma$. Jets are defined using the k_T -algorithm [21]. The rapidities refer to the ep laboratory frame, with the HERA convention that the proton is moving towards positive rapidity.

3.1 The gluon distribution in the proton

As explained already in Section 1, an accurate knowledge of the gluon distribution in the proton is very important at the LHC because of its large gluon luminosity. At present the error on important cross sections at the LHC stemming from the gluon pdfs is about 5-7%, but can be up to 20% in certain cases. Therefore our aim is to find a region where 1) the sensitivity to the gluon in the proton is enhanced, 2) x^p is rather large, 3) the uncertainty stemming from the poorly known gluon in the *photon* is minimised.

Cut on x^γ

Requirement 3) can be assured most easily by imposing a lower cut x_{min}^γ on x^γ because at small x^γ the gluon in the photon is large. On the other hand, large values of x^γ , corresponding mainly to direct initial state photons, correspond to small values of x^p at a fixed p_T value, according to eq. (6). Therefore 2) can be achieved by a cut x_{max}^γ on x^γ . In prompt photon production, the contribution from the process $\gamma(\text{direct}) + g^p \rightarrow \gamma(\text{direct}) + \text{jet}$ is rather small anyway because this process does exist only at NLO. Therefore the subprocess $q^\gamma + g^p \rightarrow \gamma + \text{jet}$ is the one which should dominate in the region fulfilling the requirements 1)–3), and our aim is to enhance the contribution of this subprocess. To this aim we investigated how cuts on x^γ act in this respect, and found that the cut $0.05 < x_{LL}^\gamma < 0.95$ maximally enhances the sensitivity to the gluon in the proton while keeping the contribution from g^γ

³The program together with detailed documentation is available at http://www.lapp.in2p3.fr/lapth/PHOX_FAMILY/main.html.

⁴This parametrisation has been used in ref. [12] under the name AFG02.

negligible, as shown in Fig. 5. Note that the contributions ‘ g^p only’ and ‘ g^γ only’ are not disjunct, they both contain the subprocess $g^p + g^\gamma \rightarrow \gamma + \text{jet}$. This subprocess does not exist at leading order, but beyond LO its contribution is non-zero and in fact negative. This can clearly be seen in Fig. 5: The cut $0.05 < x_{LL}^\gamma < 0.95$ actually enhances the total value of the g^p -initiated part of the cross section, because the lower limit $0.05 < x_{LL}^\gamma$ removes mainly the $g^p + g^\gamma$ initiated part. The fact that the $g^p + g^\gamma$ contribution is negative also reminds us that the individual subprocesses are unphysical, such that these considerations can be viewed only as qualitative reflections of the underlying parton dynamics.

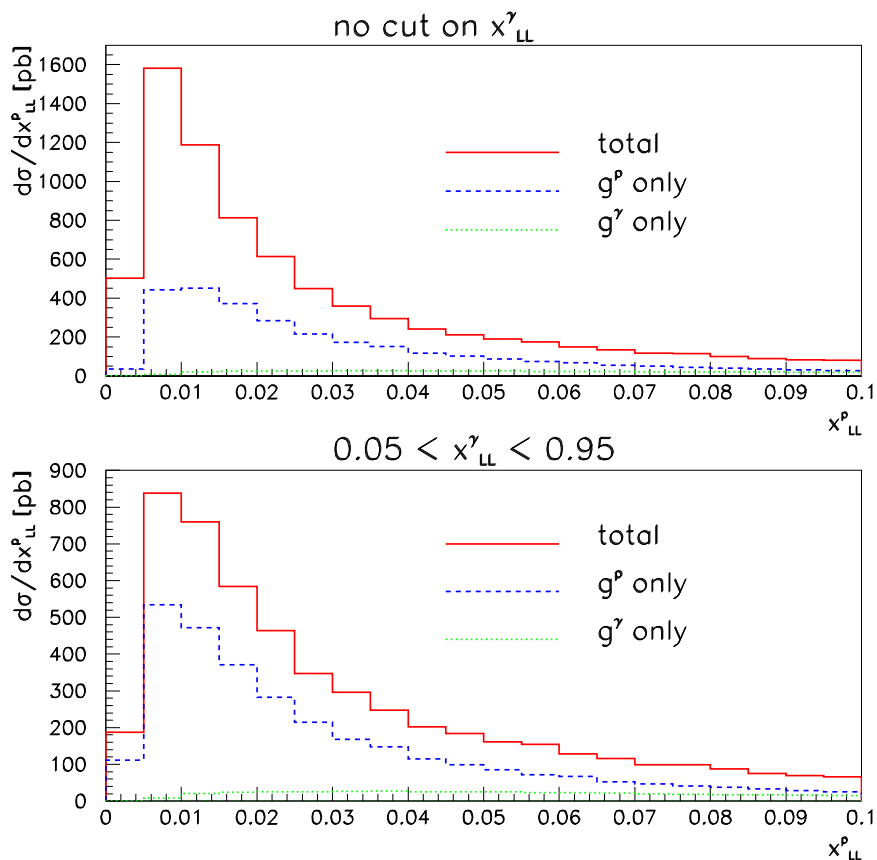


Figure 5: Effect of a cut on x_{LL}^γ to enhance the contribution of g^p initiated subprocesses

Fig. 6 shows in detail, as a function of the photon rapidity, how the requirement $0.05 < x_{LL}^\gamma < 0.95$ suppresses the direct photon contribution and enhances the relative importance of the subprocess $g^p + q^\gamma \rightarrow \gamma + \text{jet}$, especially in the region $\eta^\gamma \lesssim 1$.

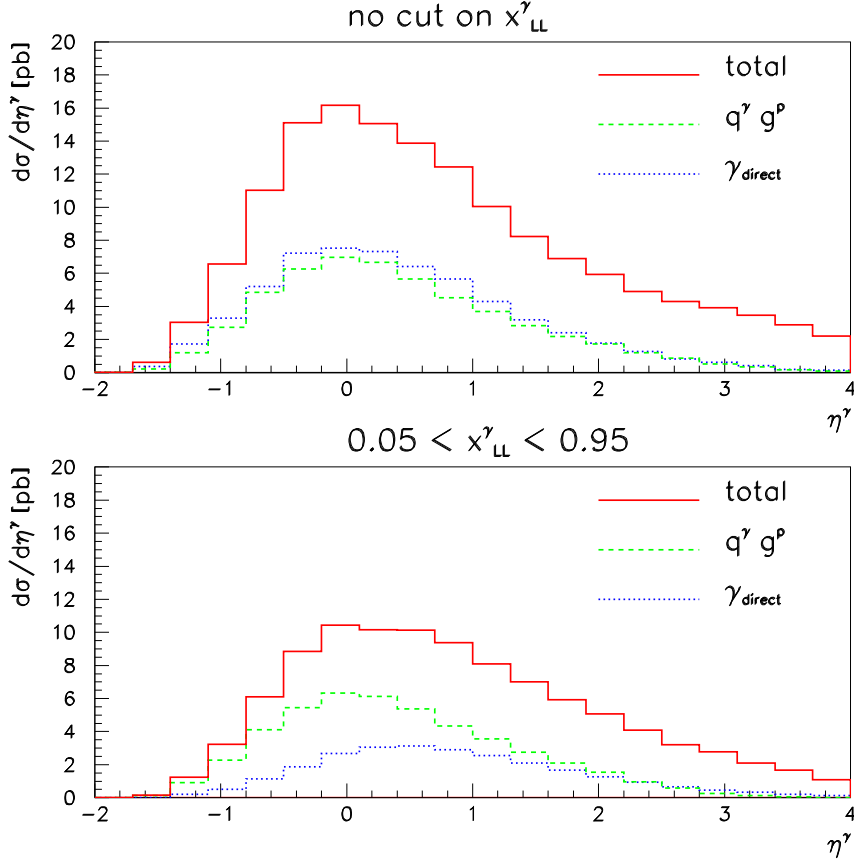


Figure 6: Relative importance of different subprocesses as a function of photon rapidity. The contribution from the direct photon gets suppressed by the cut $x_{LL}^\gamma < 0.95$.

Rapidity cuts

Another possibility to enhance the contribution of the $q^\gamma g^p$ initiated subprocesses is to impose rapidity cuts. Whereas $x_{obs,LL}$ are variables where rapidity and energy measurements enter, using rapidity cuts only is very straightforward experimentally. At small rapidities the Compton process $\gamma q^p \rightarrow \gamma q$ dominates. Further to the forward region, the importance of $q^\gamma g^p$ initiated subprocesses increases, while at very large rapidities the gluon in the photon also plays a role. Therefore, one can also meet requirements 1) to 3) by restricting the photon and jet rapidities to positive values. Fig. 7 shows that the relative contribution of g^p -initiated processes increases from about 35% of the total in the full rapidity range $-2 < \eta^{\gamma, \text{jet}} < 4$ (Fig. 7a), to about 48% in the region $0 < \eta^{\gamma, \text{jet}} < 4$, while the contribution from the gluon in the photon is still small, as can be seen from Fig. 7b. Cutting further (e.g. $1 < \eta^{\gamma, \text{jet}} < 4$) only

reduces the cross section substantially and introduces a larger uncertainty from the gluon in the photon.

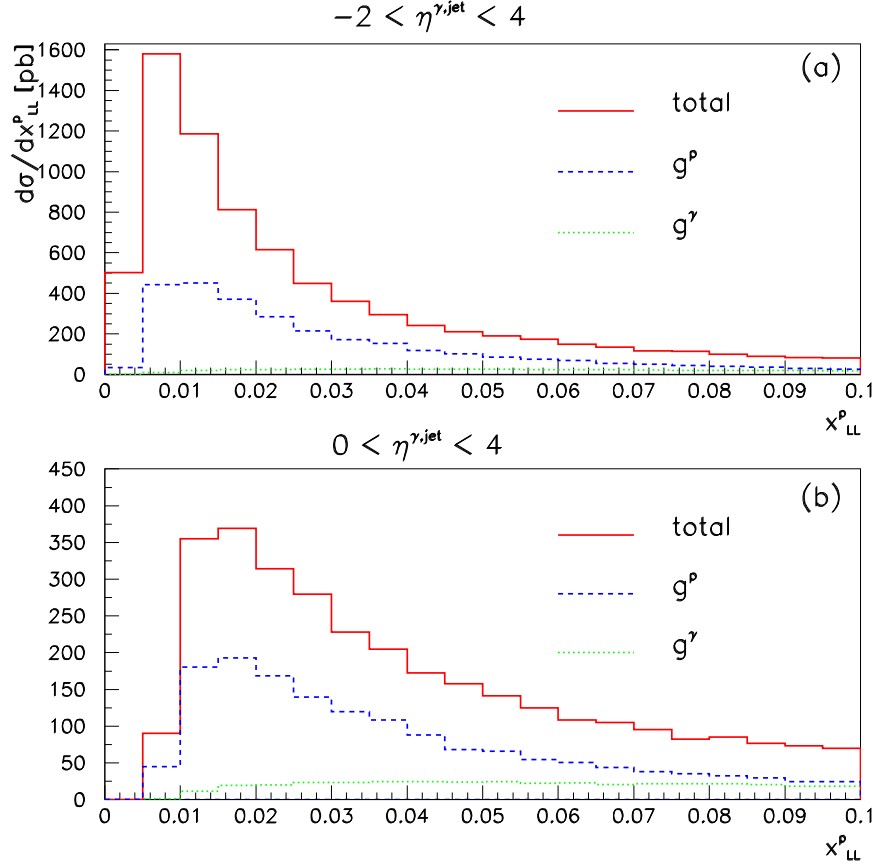


Figure 7: Restricting the rapidities to positive values enhances the relative contribution of g^p -initiated processes.

Comparing the two methods, we find that the cut $0.05 < x_{LL}^\gamma < 0.95$ reduces the total cross section only by about 31%, enhancing the contribution from the gluon in the proton from about 35% of the total to 56% of the total. The rapidity cut $0 < \eta^{\gamma, \text{jet}} < 4$ reduces the cross section by about 70% as compared to the range $-2 < \eta^{\gamma, \text{jet}} < 4$.

Scale dependence

Fig. 8 shows that the NLO cross section $d\sigma/dx_{LL}^p$ is very stable under scale changes.

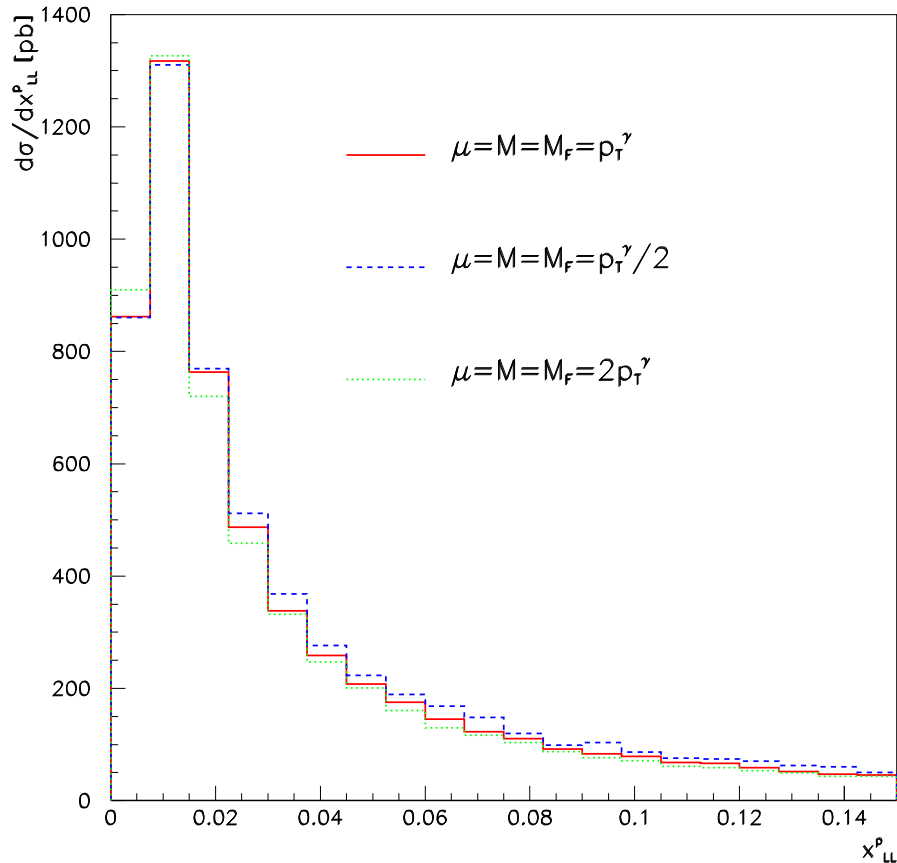


Figure 8: Scale dependence of the cross section $d\sigma/dx_{LL}^p$.

In Fig. 9, we show the predictions obtained with different parametrisations of parton distribution functions for the proton, where we chose the set CTEQ6M [22] and two different sets of MRST01 [18], the default set and the set MRST01J, which gives better agreement with the Tevatron high- E_T inclusive jet data due to a "bump" in the gluon distribution at large x .

Comparing Figs. 8 and 9, we notice that the differences in the cross sections due to different parton distribution functions are of the order of the variations due to the scale changes. However, this situation can be somewhat improved: Fig. 10 shows that the cut $0.05 < x_{LL}^p < 0.95$ makes the differences between various parametrisations more pronounced (as it enhances the gluon initiated contribution to the cross section), especially in the region $x_{LL}^p \lesssim 0.02$. On the other hand, the variation of the cross section due to scale changes in the region $x_{LL}^p \lesssim 0.015$ is not increased by the presence

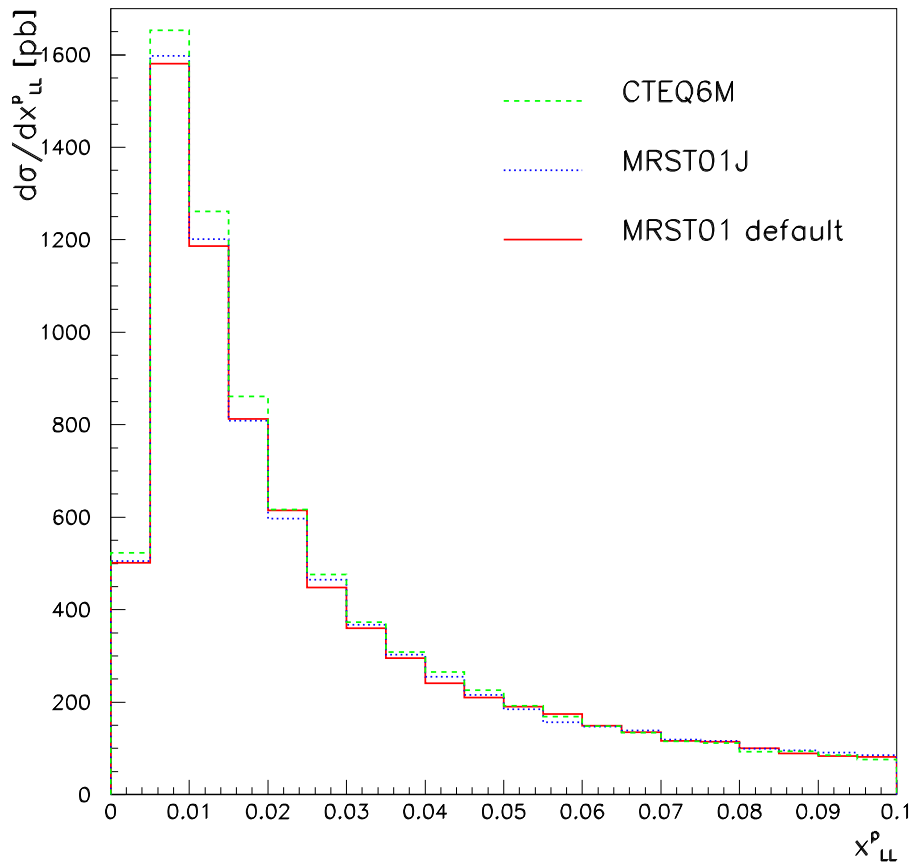


Figure 9: Dependence of the cross section $d\sigma/dx_{LL}^p$ on different parton distribution functions for the proton.

of the cut on x_{LL}^γ . Therefore, the reaction $\gamma p \rightarrow \gamma + \text{jet} + X$ could indeed be useful to further constrain the gluon in the proton in the range $x_{LL}^p \lesssim 0.015$. However, it is also clear that data with very high statistics are needed to distinguish between different parametrisations.

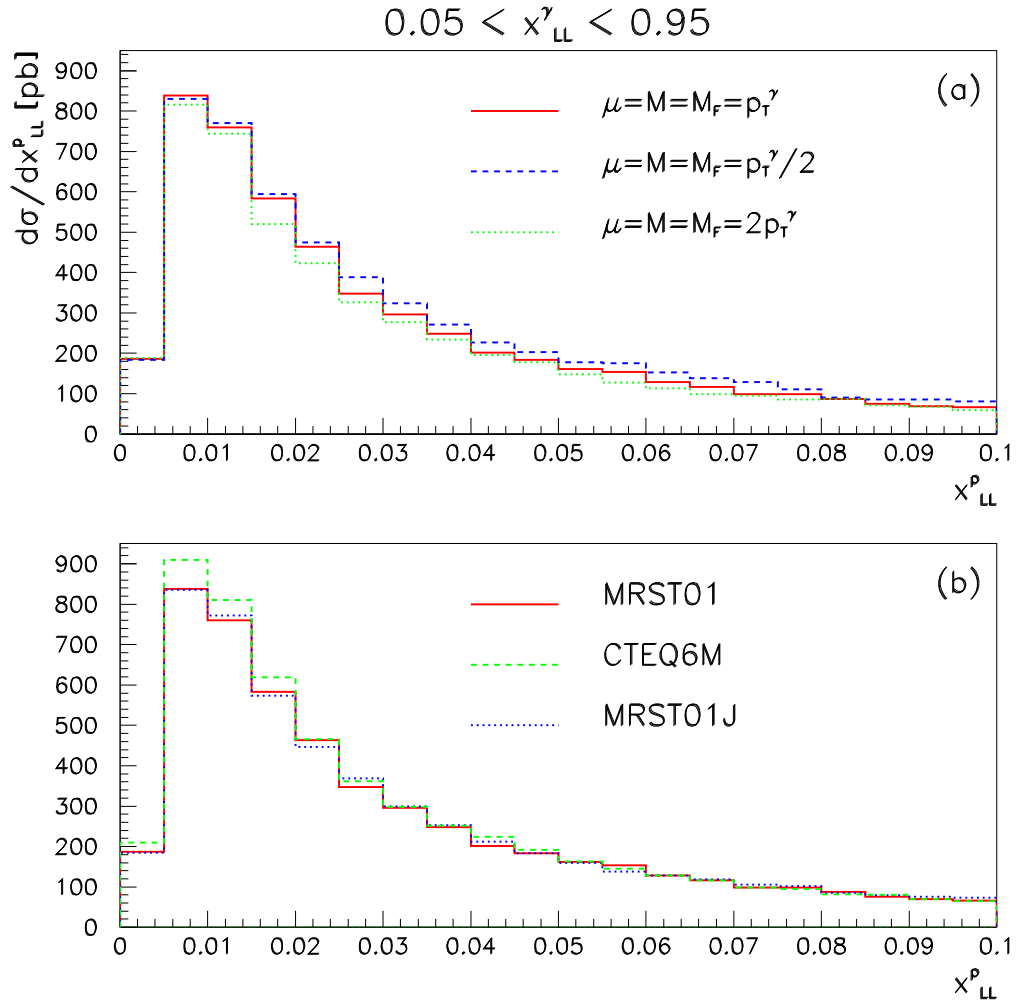


Figure 10: The cut $0.05 < x_{LL}^\gamma < 0.95$ enhances the gluon contribution and thus the differences between the parton distribution functions in the region $x_{LL}^p \lesssim 0.015$, while it does not affect the stability with respect to scale changes.

3.2 The gluon content of the photon

The photoproduction of large- p_T jets, hadrons and photons are privileged reactions to explore the gluon content of the resolved photon, which is hardly observable in $\gamma\gamma^*$ DIS. However, as discussed in the introduction, the scale dependence of the hadron and jet production cross sections is not negligible, whereas the photon cross section is more stable. This fact should allow us a more accurate determination of the gluon distribution in the photon, $g^\gamma(x^\gamma, Q^2)$.

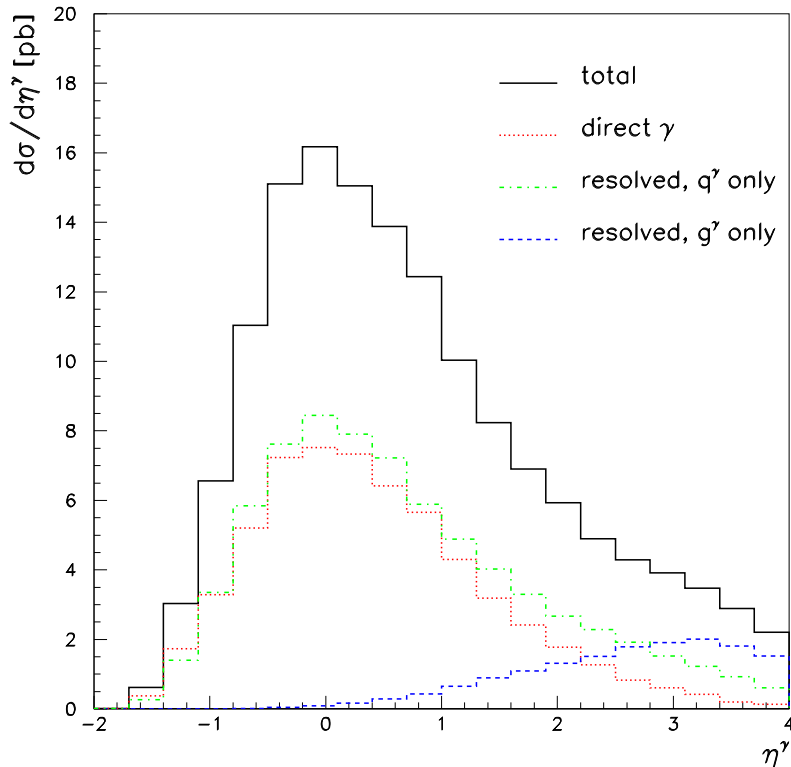


Figure 11: Magnitude of different subprocesses over the full photon rapidity range. The jet rapidities have been integrated over $-2 < \eta^{\text{jet}} < 4$, and $E_T^{\text{jet}} > 5 \text{ GeV}$, $p_T^\gamma > 6 \text{ GeV}$.

In Fig. 11 we display the various contributions to the cross section $d\sigma/d\eta^\gamma$. The gluon distribution $g^\gamma(x^\gamma, Q^2)$ only contributes at small values of x^γ , corresponding to large values of η^γ , and we shall try, by various cuts, to enhance the relative contribution of this component.

In Fig. 12 we see that the direct contribution, corresponding to x_{LL}^γ close to one, does not screen the contribution initiated by the gluon in the photon. But at smaller

values of x_{LL}^γ , the ‘background’ coming from other subprocesses, such as $q^\gamma g^p \rightarrow qg$, is large. Exactly this fact has been exploited to enhance the gluon from the proton by restricting x_{LL}^γ to intermediate values, see Fig. 5. Now we would like to enhance the gluon from the *photon*, and therefore we impose a lower cut on x_{LL}^p in order to reduce the contributions from the gluon in the proton. However, this cut has no effect at very small values of x_{LL}^γ , where the gluon in the photon is most visible. Therefore, contrary to the situation for the gluon in the proton treated in the previous subsection, cuts on the photon and jet rapidities are more effective than cuts on x_{LL}^p to enhance the gluon in the photon, as shown in Fig. 13. Fig. 13 a) shows that if the photon

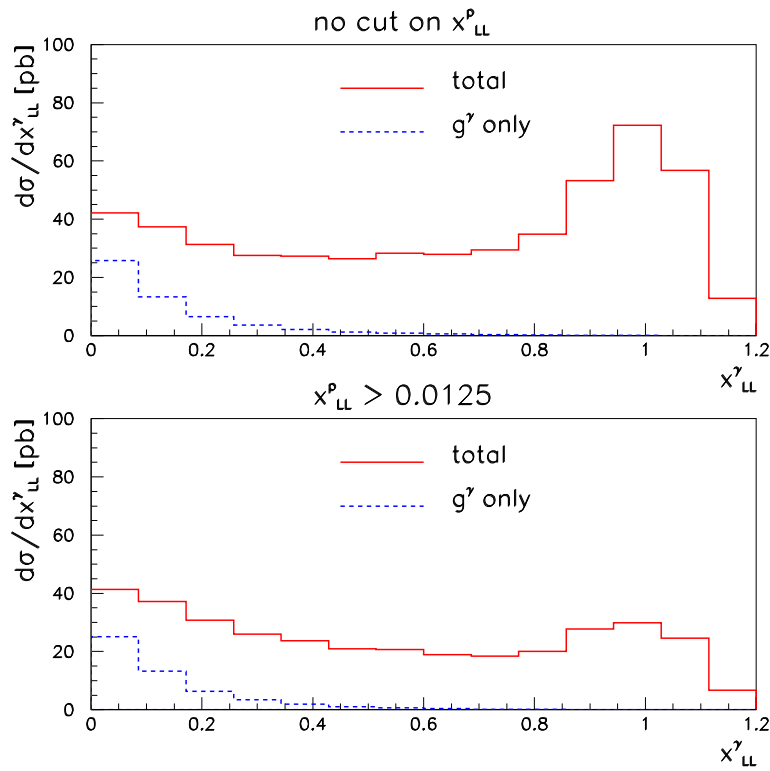


Figure 12: Effect of a lower cut on x_{LL}^p on the relative contribution from the gluon in the photon.

and jet rapidities are restricted to positive values, the resolved photon component is already fairly large, but the gluon content of the latter is still small. If we restrict the rapidities more to the forward region – especially the jet rapidity, which can be measured at larger angles – the direct photon contribution is almost completely suppressed, and the gluon contribution makes up almost 40% of the total, as shown in Fig. 13 b). Imposing even more severe cuts only decreases the cross section further

without increasing the gluon content substantially, as can be seen from Fig. 13c). Therefore the rapidity cut $\eta^\gamma > 0.5$, $\eta^{\text{jet}} > 1.5$ seems to be the optimal compromise between enhancement of the gluon content and reduction of the cross section.

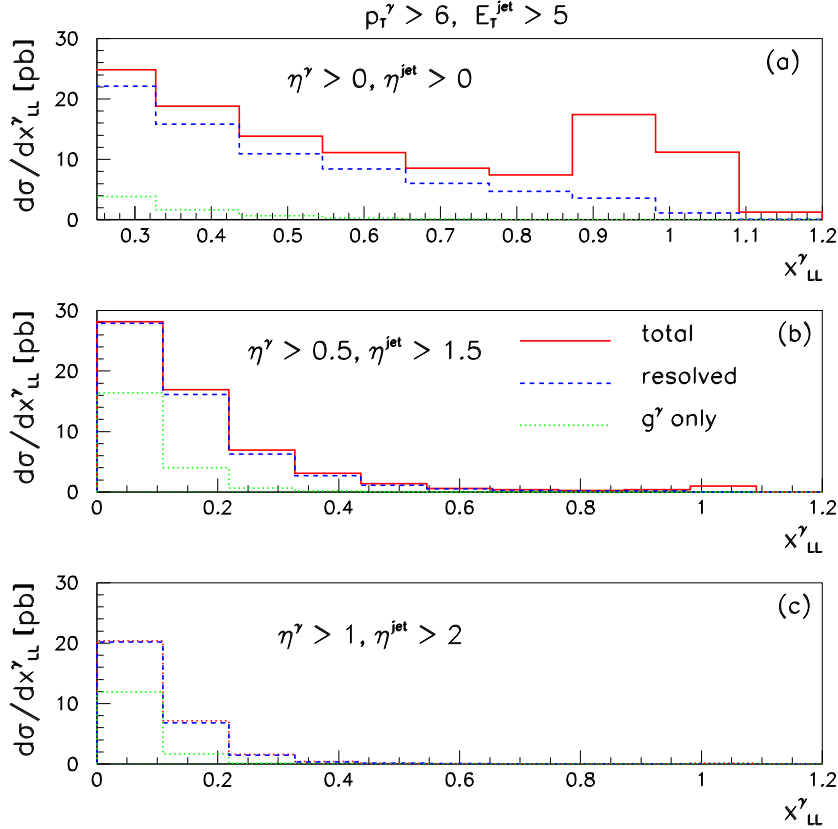


Figure 13: Effect of rapidity cuts to enhance the contribution from the gluon in the photon.

Note that the lower cuts on the transverse momenta are rather large, $p_T^\gamma > 6$ GeV, $E_T^{\text{jet}} > 5$ GeV. One can increase the cross section by choosing lower p_T cuts, as shown in Fig. 14. This figure also shows the scale dependence of $d\sigma/dx_{LL}^\gamma$ in the presence of the cuts $\eta^\gamma > 0, \eta^{\text{jet}} > 0$ respectively $\eta^\gamma > 0.5, \eta^{\text{jet}} > 1.5$. The behaviour of the cross section $d\sigma/dx_{LL}^\gamma$, which varies by $\pm 8\%$ under the scale changes, is less good than the behaviour of $d\sigma/dx_{LL}^p$ (see Fig. 8). However, one should keep in mind that the distribution g^γ is poorly known and that a determination of the latter with an accuracy of $\pm 10\%$ would already be welcome.

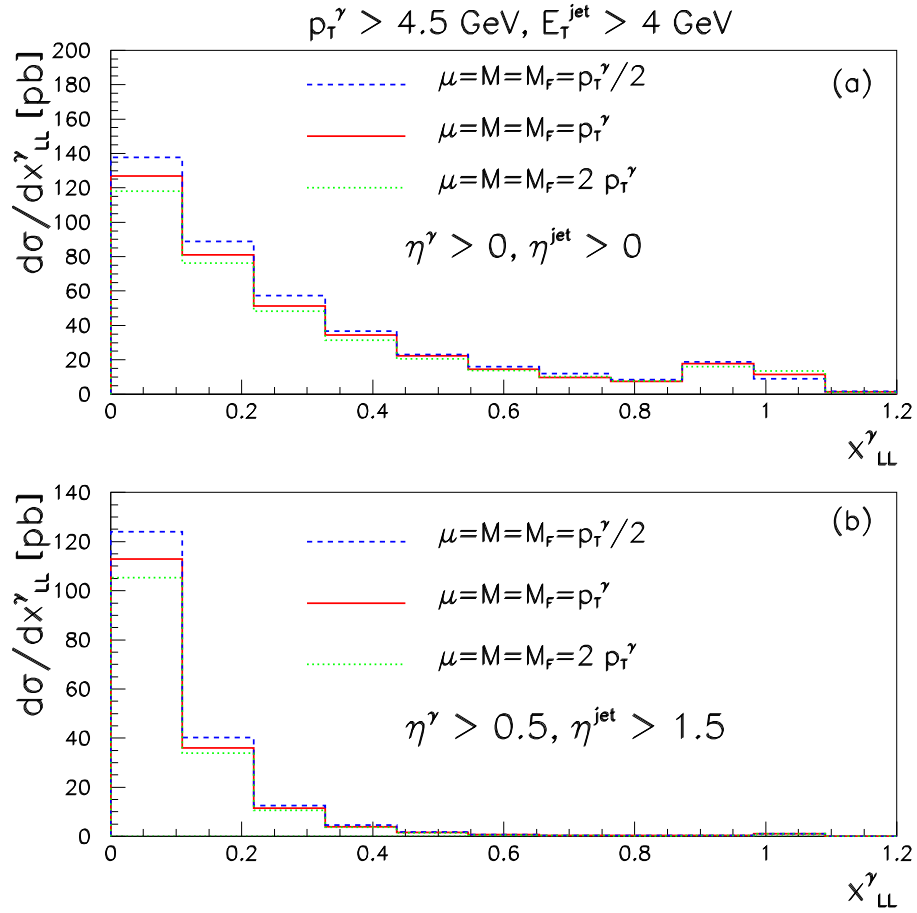


Figure 14: Scale dependence of $d\sigma/dx_{LL}^\gamma$ in the presence of forward rapidity cuts.

4 Conclusions

In this work we studied the possibility to measure the gluon distribution in the proton and in the photon by means of the reaction $\gamma + p \rightarrow \gamma + \text{jet} + X$. This reaction is well suited for such a study because of the stability of the theoretical prediction under variations of the renormalisation and factorisation scales, and because the prompt photon cross section does not suffer from large uncertainties due to hadronisation in the final state.

We have shown that gluon induced subprocesses give important contributions to the cross section in the x -ranges $0 < x_{LL}^p \lesssim 0.1$ for the proton and $0 < x_{LL}^\gamma \lesssim 0.2$ for the photon.

The effects of cuts on x_{LL}^γ respectively x_{LL}^p , or on the pseudo-rapidities η^γ and η^{jet} , are investigated in detail. We found that a judicious choice of cuts allows us to enhance the ‘signals’, i.e. the gluon induced subprocesses, over the ‘background’ stemming from other subprocesses, to constitute up to $\sim 50\%$ of the total cross section.

However, the relevant cross sections are small, of the order of 10 - 50 pb. Clearly these numbers require a large luminosity to obtain observable effects.

Acknowledgements

GH would like to thank the LPT Orsay and the LAPTH Annecy for their hospitality while part of this work has been completed, and also Günter Grindhammer for encouragement to pick up again the subject of asymmetric cuts.

References

- [1] J. Breitweg *et al.* [ZEUS Collaboration], Phys. Lett. B **472** (2000) 175 [hep-ex/9910045];
J. Breitweg *et al.* [ZEUS Collaboration], Phys. Lett. B **413** (1997) 201 [hep-ex/9708038].
- [2] S. Chekanov *et al.* [ZEUS Collaboration], Phys. Lett. B **511** (2001) 19 [hep-ex/0104001].
- [3] H1 Collaboration, submitted to the Int. Europhysics Conference on High Energy Physics, EPS03, July 2003, Aachen (Abstract 093), and to the XXI Int. Symposium on Lepton and Photon Interactions, LP03, August 2003, Fermilab.
- [4] L. E. Gordon, Phys. Rev. D **57** (1998) 235 [hep-ph/9707464].
- [5] M. Fontannaz, J. P. Guillet and G. Heinrich, Eur. Phys. J. C **21** (2001) 303 [hep-ph/0105121].

- [6] M. Fontannaz, J. P. Guillet and G. Heinrich, Eur. Phys. J. C **22** (2001) 303 [hep-ph/0107262].
- [7] M. Krawczyk and A. Zembrzuski, Phys. Rev. D **64** (2001) 114017 [hep-ph/0105166].
- [8] A. Zembrzuski and M. Krawczyk, hep-ph/0309308.
- [9] M. Klasen, Rev. Mod. Phys. **74** (2002) 1221 [hep-ph/0206169].
- [10] C. Adloff *et al.* [H1 Collaboration], DESY-02-225, hep-ex/0302034.
- [11] B. A. Kniehl, G. Kramer and B. Pötter, Nucl. Phys. B **597** (2001) 337 [hep-ph/0011155].
- [12] M. Fontannaz, J. P. Guillet and G. Heinrich, Eur. Phys. J. C **26** (2002) 209 [hep-ph/0206202].
- [13] R. Lemrani [H1 Collaboration], *Talk given at 11th International Workshop on Deep Inelastic Scattering (DIS 2003), St. Petersburg, Russia, 23-27 Apr 2003*, hep-ex/0308066;
R. Lemrani-Alaoui, “*Prompt photon production at HERA*”, Ph.D. thesis, DESY-THESIS-2003-010, available at http://www-h1.desy.de/publications/theses_list.html.
- [14] P. Aurenche, L. Bourhis, M. Fontannaz and J. P. Guillet, Eur. Phys. J. C **17** (2000) 413 [hep-ph/0006011].
- [15] S. Frixione, Phys. Lett. B **429** (1998) 369 [hep-ph/9801442].
- [16] S. Frixione and G. Ridolfi, Nucl. Phys. B **507** (1997) 315 [hep-ph/9707345].
- [17] J. Chyla and K. Sedlak, hep-ph/0308116.
- [18] A. D. Martin, R. G. Roberts, W. J. Stirling and R. S. Thorne, Eur. Phys. J. C **23** (2002) 73 [hep-ph/0110215].
- [19] P. Aurenche, J. P. Guillet and M. Fontannaz, Z. Phys. C **64** (1994) 621;
P. Aurenche, J. P. Guillet and M. Fontannaz, new version of AFG, publication in preparation.
- [20] L. Bourhis, M. Fontannaz and J. P. Guillet, Eur. Phys. J. C **2** (1998) 529 [hep-ph/9704447].
- [21] S. Catani, Y. L. Dokshitzer, M. H. Seymour and B. R. Webber, Nucl. Phys. B **406** (1993) 187;
S. D. Ellis and D. E. Soper, Phys. Rev. D **48** (1993) 3160 [hep-ph/9305266].

- [22] J. Pumplin, D. R. Stump, J. Huston, H. L. Lai, P. Nadolsky and W. K. Tung, JHEP **0207** (2002) 012 [hep-ph/0201195].